

## Optical Measurements of $\Delta\text{pH}$ and $\Delta\psi$ in Corn Root Membrane Vesicles: Kinetic Analysis of $\text{Cl}^-$ Effects on a Proton-Translocating ATPase

Alan B. Bennett and Roger M. Spanswick

Section of Plant Biology, Division of Biological Sciences, Cornell University, Ithaca, N.Y. 14853

**Summary.** The optical probes 9-aminoacridine, quinacrine, and bis (3-propyl-5-oxoisoxazol-4-yl) pentamethine oxonol (OX-VI) were used to measure the formation of pH and electric potential gradients in vesicles believed to be derived from corn root tonoplast membranes. Under certain conditions the quenching of fluorescence of 9-aminoacridine was shown to be quantitatively related to  $\Delta\text{pH}$ , and the shift in the absorbance spectrum (measured as absorbance difference at 610 and 580 nm) of OX-VI shown to be quantitatively related to  $\Delta\psi$ . In the absence of chloride ions, a positive interior membrane potential of approximately +100 mV was formed upon the addition of 5 mM Mg/ATP to a suspension of membrane vesicles. The addition of  $\text{Cl}^-$  salts reduced  $\Delta\psi$  and stimulated the formation of  $\Delta\text{pH}$ . In the presence of 50 mM  $\text{Cl}^-$ , a  $\Delta\text{pH}$  of approximately 1.1 units was established following the addition of 5 mM Mg/ATP. The kinetics of  $\text{Cl}^-$  activation of  $\text{H}^+$  transport could be resolved into a linear and a saturable component, with a  $K_m$  for the saturable component between 4 and 5 mM.  $\text{Cl}^-$  inhibition of  $\Delta\psi$  showed similar kinetics, indicating that  $\text{Cl}^-$  activates electrogenic  $\text{H}^+$  transport as a permeant anion. The biphasic kinetics suggest two pathways for  $\text{Cl}^-$  permeation, with the linear component attributable to permeation through the lipid bilayer and the saturable component attributable to permeation through an anion channel. This model is supported by the effects of the anion channel blockers, 4-acetamido-4'-isothiocyano-2,2'-stilbenedisulfonic acid (SITS) and 4,4'-diisothiocyano-2,2'-stilbenedisulfonic acid (DIDS), which abolished the saturable component but not the linear component of  $\text{Cl}^-$  stimulated  $\text{H}^+$  transport.

$\text{Cl}^-$  also stimulated ATPase activity associated with the membrane vesicles both in the absence and presence of gramicidin. In the presence of gramicidin the kinetics of  $\text{Cl}^-$  stimulation of ATPase activity were adequately described by a Michaelis-Menten function with a  $K_m$  for  $\text{Cl}^-$  between 4 and 5 mM. This result indicated a direct role for  $\text{Cl}^-$  in activating the  $\text{H}^+$ -ATPase in addition to its apparent role as a permeant anion. The similarity in  $K_m$  values for  $\text{Cl}^-$  stimulation of the ATPase and for the saturable component of  $\text{Cl}^-$  stimulation of  $\text{H}^+$  transport suggests that the  $\text{H}^+$ -ATPase may be closely associated with a  $\text{Cl}^-$  channel and that together they catalyze the nearly electroneutral transport of  $\text{H}^+$  and  $\text{Cl}^-$  *in vivo*.

**Key Words**  $\text{H}^+$ -ATPase ·  $\text{Cl}^-$  activation · DIDS inhibition · electrogenic transport · membrane vesicles · tonoplast · corn roots

## Introduction

Following the identification of ionophore-stimulated ATPase activity in a population of tobacco callus microsomal vesicles (Sze, 1980), evidence has rapidly accumulated supporting the existence of an electrogenic, proton-translocating ATPase in the microsomal membrane fraction obtained from higher plant tissues (Hager, Frenzel & Laible, 1980; Rasi-Caldogno, DeMichelis & Pugliarello, 1981; Sze & Churchill, 1981; DuPont, Bennett & Spanswick, 1982a; Mettler, Mandala & Taiz, 1982; Stout & Cleland, 1982). It has been suggested that the  $\text{H}^+$ -ATPase is associated with vesicles derived from plasma membrane (Sze & Churchill, 1981; Stout & Cleland, 1982), endoplasmic reticulum (Hager et al., 1980) or tonoplast (Mettler et al., 1982). In a separate paper we have demonstrated that the proton-translocating ATPase in corn root homogenates could be completely separated from plasma membrane and mitochondrial markers, and equilibrated at a density identical to that of tonoplast on sucrose gradients (DuPont, Bennett & Spanswick, 1982b). The ionic requirements determined for the  $\text{H}^+$ -ATPase from corn roots (DuPont, Giorgi & Spanswick, 1982c) were also similar to those of an ATPase described in purified beet root vacuoles (Walker & Leigh, 1981), providing further evidence that the activity present in corn root homogenates and possibly other plant tissue is associated with tonoplast vesicles.

In a preliminary paper we reported that ATP-dependent proton transport was stimulated by  $\text{Cl}^-$  and  $\text{Br}^-$  (DuPont et al., 1982a). This stimulation of ATP-dependent  $\text{H}^+$  transport by permeant anions suggested that the  $\text{H}^+$ -ATPase catalyzed an electrogenic influx of

protons and that the formation of a pH gradient ( $\Delta\text{pH}$ ) was impeded by a positive interior membrane potential ( $\Delta\psi$ ) in the absence of permeant ions. In this paper, the effects of  $\text{Cl}^-$  on both the formation of  $\Delta\text{pH}$  and  $\Delta\psi$  as well as ATPase activity are presented. The use of fluorescent amine dyes permitted a kinetic evaluation of  $\text{Cl}^-$  stimulation of initial rates of  $\text{H}^+$  transport, with results indicating that the  $\text{H}^+$ -ATPase is directly activated by  $\text{Cl}^-$  and that the  $\text{H}^+$ -ATPase may be closely associated with a  $\text{Cl}^-$  channel.

## Materials and Methods

### Preparation of Vesicles

Sealed microsomal vesicles were prepared as previously described (DuPont et al., 1982a). Briefly, 1.5 cm corn root tips were excised and homogenized in 0.25 M sorbitol, 2 mM EGTA, 0.1%  $\beta$ -mercaptoethanol, 0.1% bovine serum albumin (BSA), and 25 mM Bis-tris-propane/Mes (pH 7.4). A microsomal pellet (10,000–80,000  $\times g$  pellet) was resuspended and layered on a 10% dextran T-70 cushion and centrifuged at 80,000  $\times g$  for 1 hr. Vesicles collected at the dextran interface were used for all subsequent assays. Detailed characterization of this fraction has been described elsewhere (DuPont et al., 1982b).

### Fluorescence Assays

Acid interior pH gradients were measured as quenching of fluorescence of the permeant amine dyes, 9-aminoacridine and quinacrine. Vesicles, appropriate salts, and either 9-aminoacridine or quinacrine were added to an assay buffer of 0.25 M sorbitol, and 25 mM Bis-tris-propane/Mes (pH 6.75) to give a final volume of 1.5 ml and a final dye concentration of 10  $\mu\text{M}$ . Typically 100–200 or 400–600  $\mu\text{g}$  membrane protein were added for assays with quinacrine and 9-aminoacridine, respectively. Fluorescence was measured at room temperature (approx. 25°C) with a Varian 634 spectrophotometer equipped with a total fluorescence attachment and the output recorded with an MFE chart recorder after passing through an R/C filter with a time constant of 0.75 sec. Emission was measured through a green band pass filter (460–650 nm window) and excitation was at 423 nm with 9-aminoacridine and 440 nm with quinacrine. Measurements of ATP-dependent  $\text{H}^+$  influx were initiated by the addition of 15  $\mu\text{l}$  of 0.5 M Bis-tris-propane/ATP (pH 6.75). Gramicidin was dissolved in methanol and when used resulted in a final concentration of 0.2% methanol. SITS and DIDS were added from aqueous stock solutions.

### Absorption Spectroscopy of OX-VI

Absorption changes of bis(3-propyl-5-oxoisoxazol-4-yl)pentamethine oxonol (OX-VI) were measured with a dual wavelength absorption spectrophotometer (constructed by Dr. R.K. Clayton, Cornell University) equipped with two Jobin-Yvon monochrometers set at 610 and 580 nm. The

photomultiplier output was connected to a Princeton Applied Research lock-in amplifier and the output recorded with an MFE chart recorder. The time constant on the lock-in amplifier was typically set at 1.0 or 3.0 sec. Assays were performed in 2.5 ml final volume of 2.5  $\mu\text{M}$  OX-VI, 0.25 M sorbitol, 25 mM Bis-tris-propane/Mes (pH 6.75), 5 mM  $\text{MgSO}_4$ , and other salts as indicated. Additions of Bis-tris-propane/ATP (pH 6.75),  $\text{H}_2\text{SO}_4$ , or gramicidin were made through an injection port. Since the addition of ATP itself caused a shift in  $A_{(610-580)}$ , all data were calculated, and presented, relative to a baseline recorded after dissipation of  $\Delta\psi$  by the addition of either 2  $\mu\text{M}$  gramicidin or 4 mM KSCN.

### ATPase Assays

ATPase activity was assayed at 25°C for either 20 or 30 min with 30–50  $\mu\text{g}$  membrane protein per assay. ATPase activity, under the conditions used, was linear for 30 min and less than 5% of the ATP was hydrolyzed during this period. The final assay consisted of 25 mM Bis-tris-propane/Mes (pH 6.75), 5 mM Bis-tris-propane ATP, 25 mM sorbitol, and appropriate salts in a final volume of 0.5 ml. Phosphate was determined by the method of Ames (1966). Typically, the reaction was started by the addition of 50  $\mu\text{l}$  vesicles to each test tube at 15 sec intervals, and the reaction stopped by the addition of the ammonium-molybdate reagent to each tube at 15 sec intervals. After color development (approx. 45 min) absorbance at 820 nm was measured with a Varian 634 spectrophotometer at 15 sec intervals. Interference by 25 mM sorbitol was slight, and equal amounts of sorbitol were included in all phosphate standards.

### Proteins

Proteins were measured by the method of Bradford (1976) using a commercially available reagent (Bio-Rad Laboratories, Richmond, Calif.) and bovine gammaglobulin as standard.

### Chemicals

ATP was obtained from Boehringer Mannheim (Indianapolis, Ind.) as the disodium salt. The sodium was routinely removed from ATP solutions by passage through Dowex 50W and the pH of the resulting solution adjusted with solid Bis-tris-propane to 6.75. Gramicidin was from Calbiochem-Boehringer (La Jolla, Calif.), OX-VI from Molecular Probes Inc. (Plano, Texas), and all other chemicals from Sigma Chemical Co. (St. Louis, Mo.).

## Results and Discussion

### Initial Rates of $\text{H}^+$ Transport

Quenching of fluorescence of the amine dyes, 9-aminoacridine and quinacrine was used to measure ATP-dependent  $\text{H}^+$  transport into membrane vesicles of corn roots. These probes of

$\Delta\text{pH}$  have been well characterized in artificial lipid vesicles (Deamer, Prince & Crofts, 1972) and successfully used with biologically derived membrane vesicles (Lee & Forte, 1978; Brey & Rosen, 1979). The quenching of fluorescence of both dyes upon the addition of ATP to a suspension of corn root membrane vesicles is shown in Fig. 1. The same amount of protein was present for both assays. With 9-aminoacridine a rapid decrease in fluorescence was observed upon the addition of ATP which occurred even in the absence of membrane vesicles and is due to the formation of a nonfluorescent complex of 9-aminoacridine with ATP (Bashford & Thayer, 1977). This initial decrease was followed by a slower quenching which was reversed by the addition of  $2\mu\text{M}$  nigericin. Quinacrine apparently does not complex with ATP and only the slow, reversible quenching of fluorescence was observed. The increased sensitivity of quinacrine is apparent in Fig. 1 and for this reason was utilized in early characterization of  $\text{H}^+$  transport in these vesicles (DuPont et al., 1982a).

Upon addition of ATP, the initial decrease in fluorescence is linear for approximately 3 min and then begins to level off. We have interpreted this as an interaction between the active influx of  $\text{H}^+$ , dependent on ATP, and the passive efflux. We have previously shown that after fluorescence quenching had leveled off, the passive leak became apparent when ATP levels were reduced by the addition of hexokinase and glucose (DuPont et al., 1982a). By this interpretation measurements of the initial rate of fluorescence quench reflect the activity of the  $\text{H}^+$ -ATPase whereas measurements of the total quench reflect the interaction between the  $\text{H}^+$  pump and  $\text{H}^+$  leak.

The relatively low rate of fluorescence quenching in these vesicles permitted measurements of initial rates of quench and suggested that these rates could be useful in kinetic analyses of initial rates of  $\text{H}^+$  transport. In this regard it was important to determine whether the dye response was linear with protein concentration and this was verified for both quinacrine and 9-aminoacridine (Fig. 2). The difference in slopes of the lines for quinacrine and 9-aminoacridine again demonstrates the nearly sixfold greater sensitivity of quinacrine as compared to 9-aminoacridine.

It was also necessary to determine under what conditions these probes responded to  $\Delta\text{pH}$  in an ideal fashion. Since 9-aminoacridine

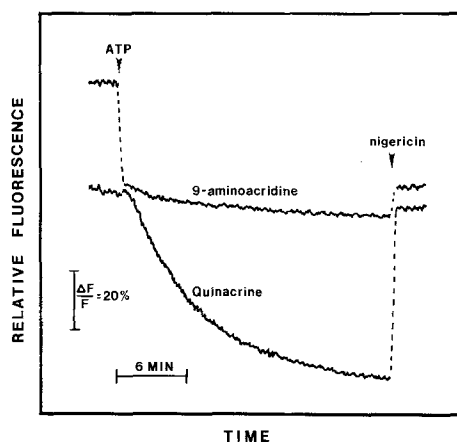
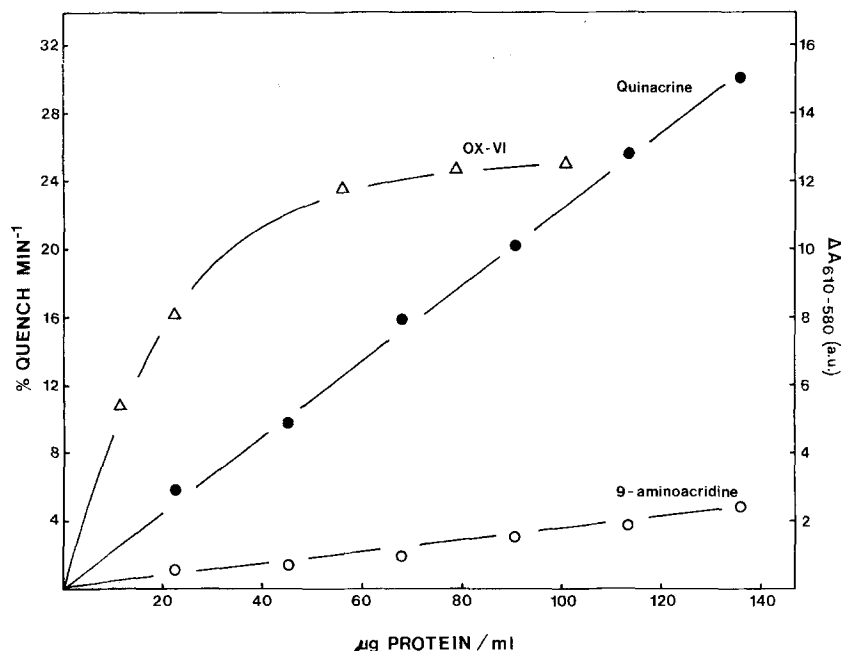


Fig. 1. Comparison of the time course of fluorescence quenching of 9-aminoacridine and quinacrine. Membrane vesicles (125  $\mu\text{g}$  protein) were incubated in 1.5 ml of 0.25 M sorbitol, 25 mM Bis-tris-propane/Mes (pH 6.75), 5 mM  $\text{MgSO}_4$ , 50 mM KCl, and either 10  $\mu\text{M}$  9-aminoacridine or quinacrine. Addition of 15  $\mu\text{l}$  0.5 M Bis-tris-propane/ATP or 3  $\mu\text{l}$  1 mM nigericin in methanol were made at the indicated points

has been reported to be a reliable quantitative indicator of  $\Delta\text{pH}$  (Deamer et al., 1972; Schuldiner, Rottenberg & Avron, 1972) the quenching of fluorescence of this dye in response to an imposed  $\Delta\text{pH}$  was determined. The left panel of Fig. 3 shows a schematic diagram of the partitioning of 9-aminoacridine into membrane vesicles. Also shown in this panel is the quantitative description of the partitioning of a permeant amine in response to  $\Delta\text{pH}$  (Eq. 1), where  $(\text{AH})_i$  and  $(\text{AH})_o$  are the concentrations of the protonated amine inside and outside of the vesicles, respectively. The following two equations (Eqs. 2 and 3), developed by Deamer et al. (1972), substitute easily measurable values of fluorescence quenching for  $(\text{AH})_i$  and  $(\text{AH})_o$ , where %Q is the percent quenching of fluorescence and  $V_i$  and  $V_o$  are internal and external volumes, respectively. This substitution makes the assumption that internalized amine is not fluorescent.

In order to test the quantitative response of 9-aminoacridine to  $\Delta\text{pH}$  it was necessary to impose an acid interior pH gradient of measurable magnitude, and record the resulting quenching of fluorescence. The right panel of Fig. 3 shows such an experiment, where membrane vesicles were allowed to equilibrate with a 2.5 mM Bis-tris-propane/Mes (pH 6.75) buffer and then small volumes of 1 N NaOH added to raise the external pH. Following this base-pulse the fluorescence of 9-aminoacridine was



**Fig. 2.** Effect of membrane protein concentration on the response of 9-aminoacridine, quinacrine, and OX-VI. Initial rates of fluorescence quenching of 9-aminoacridine (○) or quinacrine (●) were measured under the conditions described in Fig. 1. Shifts in the absorbance difference at 610 and 580 nm of OX-VI were measured in 2.5 ml of 25 mM Bis-tris-propane/Mes (pH 6.75), 5 mM  $\text{MgSO}_4$ , and 2.5  $\mu\text{M}$  OX-VI (Δ). After recording a stable baseline the peak absorbance change following the addition of 25  $\mu\text{l}$  0.5 M Bis-tris-propane-ATP was recorded

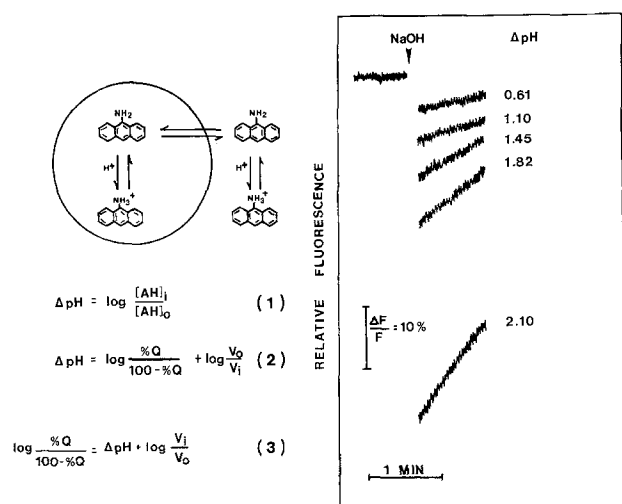


**Fig. 3.** Fluorescence quenching of 9-aminoacridine in response to an imposed pH gradient. *Left*, a schematic diagram of the partitioning of 9-aminoacridine into membrane vesicles and a quantitative description of the quenching of fluorescence in response to  $\Delta \text{pH}$  as in Deamer et al. (1972). *Right*, experimental conditions as in Fig. 1 with 10  $\mu\text{M}$  9-aminoacridine. Acid interior pH gradients imposed by additions of 2.5–13  $\mu\text{l}$  1 N NaOH. Measurements of pH in the cuvette before and after addition of NaOH were used to calculate  $\Delta \text{pH}$

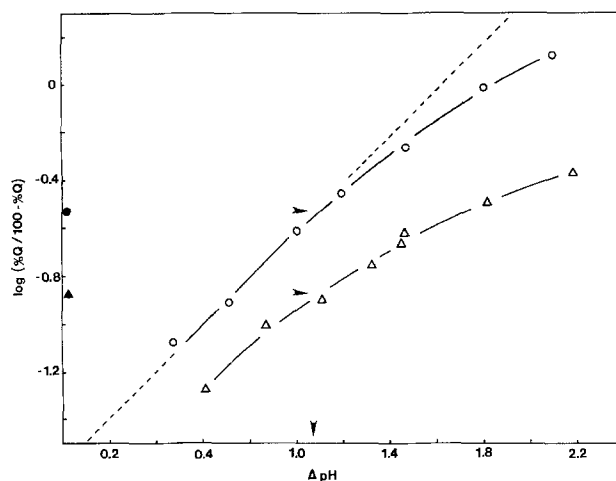


**Fig. 4.** Plot of  $\log(\%Q/100 - \%Q)$  as a function of imposed  $\Delta \text{pH}$  at two concentrations of membrane protein, measured with 9-aminoacridine. Data collected as in Fig. 3 with membrane vesicles present at a final concentration of 400  $\mu\text{g}$  membrane protein/ml (○), or 133  $\mu\text{g}$  membrane protein/ml (Δ). Points (●) and (▲) along the ordinate are the values of  $\log(\%Q/100 - \%Q)$  measured after addition of ATP to vesicle suspensions of 400 or 133  $\mu\text{g}$  membrane protein/ml, respectively

quenched but then began to recover. This recovery of fluorescence results from the re-equilibration of internal and external pH and has been used to measure net proton-hydroxyl permeabilities of liposomes (Nichols, Hill,

Bangham & Deamer, 1980) and membrane vesicles (Perlin & Spanswick, 1982). The magnitude of the imposed  $\Delta \text{pH}$  was calculated by measuring the pH in the cuvette before and after the addition of NaOH. The data from

similar experiments is plotted according to Eq. (3) in Fig. 4. Since Eq. (3) describes a linear relationship, a plot of the data in this form should be linear with a slope of 1, if the dye response is ideal. With high concentrations of membrane vesicles ( $400\mu\text{g}$  membrane protein/ml) and at low  $\Delta\text{pH}$  ( $<1.4$  units) the data were linear with a slope of 1 (indicated by dashed line); however at high  $\Delta\text{pH}$  the data did deviate from this line. With low concentrations of membrane vesicles ( $133\mu\text{g}$  membrane protein/ml) the data did not conform to the theoretical expectation over any range of  $\Delta\text{pH}$ . Similar results have been observed with high and low concentrations of liposomes (Deamer et al., 1972). This result indicates that 9-aminoacridine responds to  $\Delta\text{pH}$  in a quantitatively predictable fashion at high concentrations of membrane vesicles and at low  $\Delta\text{pH}$ . Since measurements of initial rates of fluorescence quenching are made over a range of low  $\Delta\text{pH}$  it was concluded that this dye, when used with  $>400\mu\text{g}$  membrane protein/ml, could be used reliably to estimate relative rates of  $\text{H}^+$  transport.

The plot of  $\log (\%Q/100 - \%Q)$  as a function of  $\Delta\text{pH}$  could also be used as a calibration curve for estimating the magnitude of  $\Delta\text{pH}$  formed in the presence of ATP. Shown in Fig. 4, on the ordinate, are the values of  $\log (\%Q/100 - \%Q)$  measured at high and low concentrations of membrane vesicles after establishment of an ATP-dependent, steady-state level  $\Delta\text{pH}$ . Only the ionophore-recoverable fluorescence quench was used to calculate  $\log (\%Q/100 - \%Q)$  for the ATP-dependent quench. These values were used along with the appropriate calibration curve, as indicated by arrows, to estimate a  $\Delta\text{pH}$  of 1.1 units. Similar experiments on three different days gave a mean estimate of  $\Delta\text{pH}$  of  $1.06 \pm 0.08$  units. These estimates assume that all vesicles capable of maintaining  $\Delta\text{pH}$  across the membrane also possess  $\text{H}^+$ -ATPase activity. Deviation from this assumption would raise the actual value of  $\Delta\text{pH}$ , so the estimates reported here are conservative.

Estimation of the intravesicular volume from the intercept of the dashed line in Fig. 4 indicates a volume of approximately  $56\mu\text{l}/\text{mg}$  membrane protein. This large volume estimate may result from the low protein content of the tonoplast or alternatively from binding or other nonideal behavior of 9-aminoacridine (Lee, Forte & Epel, 1982).

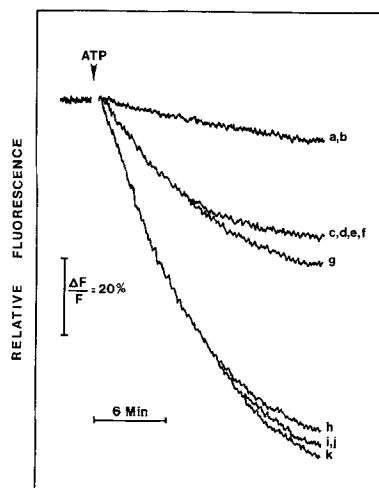


Fig. 5. Effects of  $\text{K}_2\text{SO}_4$  and various  $\text{Cl}^-$  salts on ATP-dependent quenching of quinacrine fluorescence. Experimental conditions were as in Fig. 1 with salts added as indicated. Multiple letters adjacent to single quench curves indicate overlapping curves. *a* = 5 mM  $\text{MgSO}_4$ ; *b* = 5 mM  $\text{MgSO}_4$  + 10 mM  $\text{K}_2\text{SO}_4$ ; *c* = 5 mM  $\text{MgCl}_2$ ; *d* = 5 mM  $\text{MgSO}_4$  + 10 mM  $\text{NaCl}$ ; *e* = 5 mM  $\text{MgSO}_4$  + 10 mM  $\text{LiCl}$ ; *f* = 5 mM  $\text{MgSO}_4$  + 10 mM  $\text{RbCl}$ ; *g* = 5 mM  $\text{MgSO}_4$  + 10 mM  $\text{KCl}$ ; *h* = 5 mM  $\text{MgSO}_4$  + 50 mM  $\text{NaCl}$ ; *i* = 5 mM  $\text{MgSO}_4$  + 50 mM  $\text{LiCl}$ ; *j* = 5 mM  $\text{MgSO}_4$  + 50 mM  $\text{KCl}$ ; *k* = 5 mM  $\text{MgSO}_4$  + 50 mM  $\text{RbCl}$ .

#### $\text{Cl}^-$ -Stimulation of $\text{H}^+$ Transport and $\text{H}^+$ -ATPase

A previous paper showed that  $\text{H}^+$  transport and ATPase activity were sensitive to anions and the  $\text{Cl}^-$  and  $\text{Br}^-$  were most effective in stimulating activity (DuPont et al., 1982c). Figure 5 shows that  $\text{H}^+$  transport is stimulated by  $\text{Cl}^-$  and is completely insensitive to monovalent cations. In the absence of  $\text{Cl}^-$ , 10 mM  $\text{K}_2\text{SO}_4$  had no effect on the rate of quenching of quinacrine fluorescence. When 5 mM  $\text{MgSO}_4$  was replaced with 5 mM  $\text{MgCl}_2$  or when 5 mM  $\text{MgSO}_4$  was supplemented with 10 mM  $\text{Cl}^-$  as either the  $\text{K}^+$ ,  $\text{Na}^+$ ,  $\text{Li}^+$ , or  $\text{Rb}^+$  salts, rates of quench were indistinguishable. Similar results, but higher rates of  $\text{H}^+$  transport, were obtained with 50 mM  $\text{Cl}^-$  salts.

It was likely that  $\text{Cl}^-$  stimulated  $\text{H}^+$  transport by relieving a positive interior membrane potential associated with  $\text{H}^+$ -ATPase activity, although direct activation of the  $\text{H}^+$ -ATPase by  $\text{Cl}^-$  could not be ruled out. To test these possibilities,  $\text{Cl}^-$  stimulation of ATPase activity was determined in the absence and presence of  $2\mu\text{M}$  gramicidin (Table 1). It was reasoned that the presence of gramicidin would abolish  $\Delta\text{pH}$  and

**Table 1.** Effect of cations on ATPase activity in the absence and presence of gramicidin<sup>a</sup>

Additions	ATPase activity ( $\mu\text{mol Pi/mg} \cdot \text{hr}$ )			%Salt stimu- lation
	Mg <sup>2+</sup> - depend- ent	Salt stimu- lation	Gramicidin stimu- lation	
– Gramicidin				
No salt	1.70	—	—	—
KCl	2.42	0.71	—	41.8
NaCl	2.36	0.66	—	38.7
LiCl	2.51	0.81	—	47.5
RbCl	2.61	0.91	—	53.4
+ Gramicidin				
No salt	3.21	—	1.51	—
KCl	4.69	1.47	2.27	45.9
NaCl	4.77	1.55	2.40	48.3
LiCl	4.86	1.65	2.35	51.3
RbCl	4.96	1.74	2.34	54.2

<sup>a</sup> ATPase activity assayed as in Materials and Methods with the indicated salts added at a concentration of 50 mM. Mg-ATPase is calculated as the difference in ATPase activity measured in the presence and absence of 5 mM  $\text{MgSO}_4$

$\Delta\psi$  (see Fig. 10) and only direct effects of ions on the ATPase would be apparent. In the presence of 50 mM  $\text{Cl}^-$  salts, ATPase activity was stimulated approximately 40–50% in the absence of gramicidin. In the presence of gramicidin, all rates were higher due to relief of  $\Delta\mu_{\text{H}^+}$ , but stimulation by 50 mM  $\text{Cl}^-$  salts was proportionately identical to the stimulation measured in the absence of gramicidin. This result indicates that  $\text{Cl}^-$  does not act solely as a permeant anion but has a direct role in activating the  $\text{H}^+$ -ATPase.

#### Kinetics of $\text{Cl}^-$ Stimulation of $\text{H}^+$ Transport

Since it was previously determined that 9-aminoacridine could be used reliably to measure relative initial rates of  $\text{H}^+$  transport, it was possible to determine the concentration kinetics of  $\text{Cl}^-$  stimulation of  $\text{H}^+$  transport. Using high concentrations of membrane vesicles, Fig. 6a shows the initial rates of fluorescence quench as a function of KCl concentration at either 5 or 25 mM  $\text{SO}_4^{2-}$  concentration. The kinetics could be described by:

$$V = \frac{V_{\max} \cdot S}{K_m + S} + k_u \cdot S + k_o \quad (4)$$

which describes a biphasic system with a saturable and linear phase superimposed (Cohen,

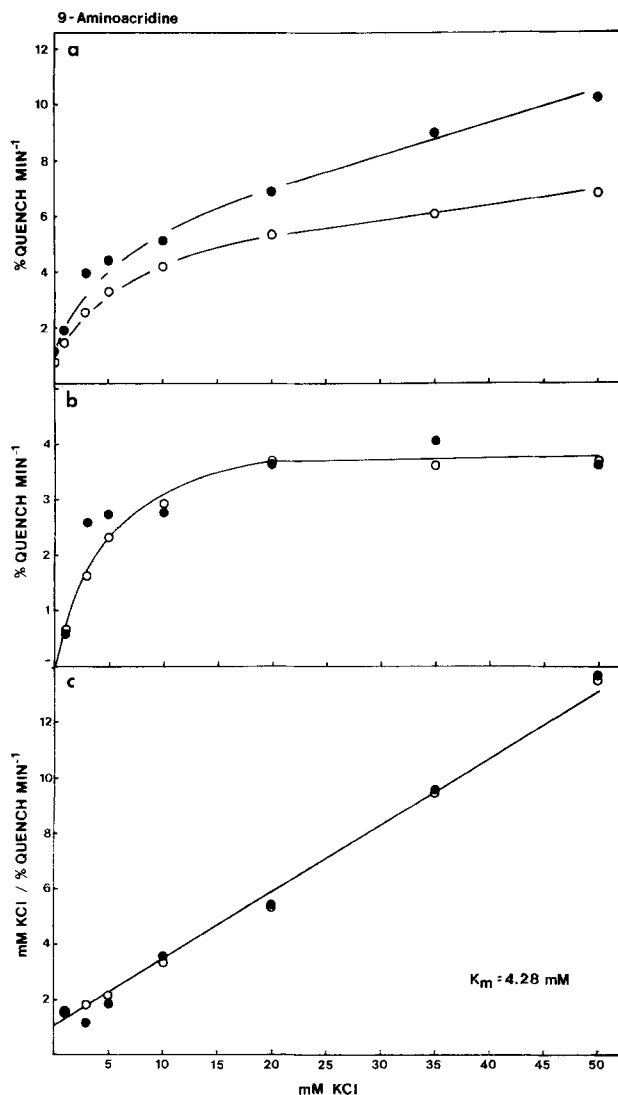


**Fig. 6.** (a): Kinetics of KCl stimulation of the initial rate of fluorescence quench of 9-aminoacridine. Experimental conditions as in Fig. 1 with 5 mM  $\text{MgSO}_4$  and 0–50 mM KCl (●), or 5 mM  $\text{MgSO}_4$ , 20 mM  $\text{K}_2\text{SO}_4$ , and 0–50 mM KCl (○). Vesicles were added to a final concentration of 550  $\mu\text{g}$  membrane protein/ml. (b): Saturable component of  $\text{Cl}^-$  stimulated rates of fluorescence quench after subtraction of the nonsaturable component as described in text. (c): Hanes-Woolf plot of data in 5(b)

1975). The slope of the linear component ( $k_u$ ) can be estimated by linear regression analysis of the points at high concentrations (20–50 mM KCl). The y-intercept for the linear component ( $k_o$ ) is merely the rate measured in the absence of KCl. When the linear component is calculated and subtracted, the residual rates define a curve which is described by a Michaelis-Menten function (Fig. 6b,c) with a  $K_m$  for  $\text{Cl}^-$  of approximately 4.3 mM.

It had been previously observed that  $\text{SO}_4^{2-}$  inhibited  $\text{H}^+$  transport (data not shown). The

kinetic analysis (Fig. 6a-c) shows that  $\text{SO}_4^{2-}$  had an effect only at high  $\text{Cl}^-$  concentrations and specifically only on the linear phases of  $\text{Cl}^-$ -stimulated  $\text{H}^+$  transport. After subtraction of the linear phases, the saturable phases of  $\text{Cl}^-$ -stimulated  $\text{H}^+$  transport in the presence of either 5 or 25 mM  $\text{SO}_4^{2-}$  were identical.

Attempts were not made to calibrate the more sensitive pH probe, quinacrine. It has been reported that this dye is not a reliable quantitative indicator of  $\Delta\text{pH}$  (Deamer et al., 1972), and could not have been calibrated by the base-pulse method due to a reported pH dependence of the dye fluorescence in free solution (Deamer et al., 1972). It was reasoned, however, that when fluorescence quenching was measured over very small  $\Delta\text{pH}$ , such as measurements of initial rates of quench, that this dye may respond linearly with  $\Delta\text{pH}$ . Since the response of this dye could not be calibrated directly, as was done with 9-aminoacridine, the experiment shown in Fig. 6a was repeated with the modifications that 10  $\mu\text{M}$  9-aminoacridine was replaced with 10  $\mu\text{M}$  quinacrine and approximately 80% less protein was used per assay. The results, shown in Fig. 7a-c, are essentially identical to those obtained with 9-aminoacridine. The  $K_m$  for the saturable component of  $\text{Cl}^-$  stimulated  $\text{H}^+$  transport estimated by either dye ranged between 4 and 5 mM  $\text{Cl}^-$  in several separate experiments. From this we concluded that initial rates of quenching of quinacrine fluorescence could also be used to measure and compare relative initial rates of  $\text{H}^+$  transport.

It was previously shown that  $\text{Cl}^-$  had a direct role in activating  $\text{H}^+$ -ATPase activity (Table 1). The kinetics of  $\text{Cl}^-$  stimulation of the  $\text{H}^+$ -ATPase were determined for comparison with the kinetics of  $\text{Cl}^-$  stimulation of  $\text{H}^+$  transport. The data, shown in Fig. 8, show simple saturation kinetics, in contrast to the bi-phasic kinetics of  $\text{Cl}^-$  stimulation of  $\text{H}^+$  transport. In agreement with Table 1,  $\text{Cl}^-$  stimulation was greater in the presence of gramicidin. The lower panel of Fig. 8 shows a Hanes-Woolf plot with indicated  $K_m$  values of approximately 2.3 and 4.4 mM for  $\text{Cl}^-$  in the absence and presence of gramicidin, respectively. In the presence of gramicidin the  $K_m$  is in close agreement with that determined for the saturable component of  $\text{Cl}^-$  stimulated  $\text{H}^+$  transport. The lower  $K_m$  determined in the absence of gramicidin was unexpected but may result from the 30-min incubation times for this assay, over which time substantial gradients of  $\Delta\text{pH}$  and/or

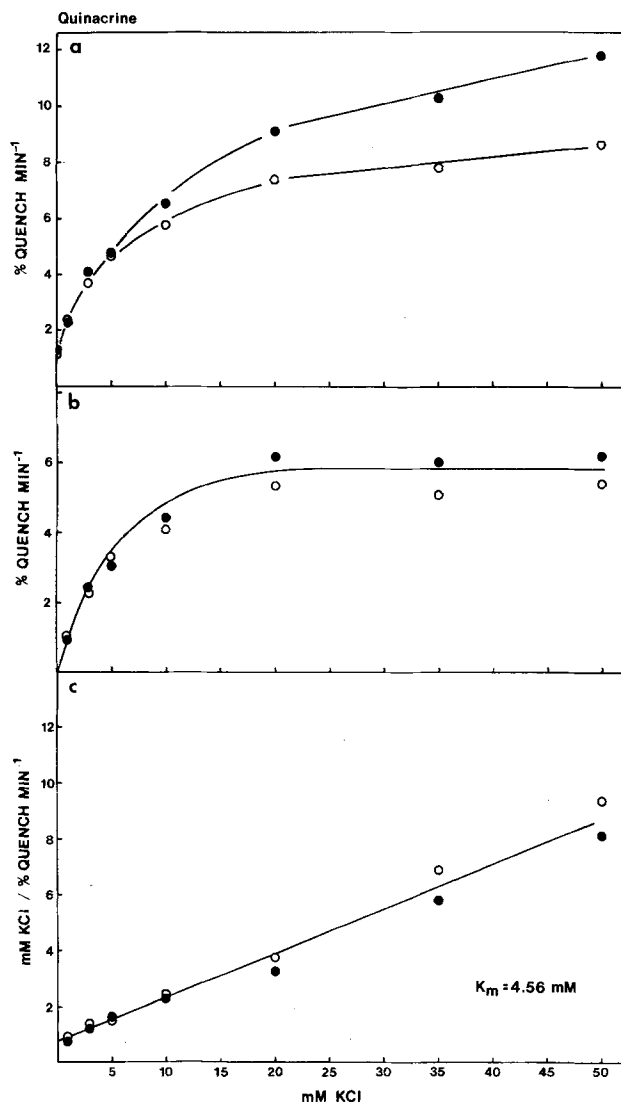


Fig. 7. (a): Kinetics of KCl stimulation of the initial rate of fluorescence quench of quinacrine. Experimental conditions as in Fig. 1 with 5 mM  $\text{MgSO}_4$  and 0–50 mM KCl (●), or 5 mM  $\text{MgSO}_4$ , 20 mM  $\text{K}_2\text{SO}_4$ , and 0–50 mM KCl (○). Vesicles were added to a final concentration of 100  $\mu\text{g}$  membrane protein/ml. (b): Saturable component of  $\text{Cl}^-$  stimulated rates of fluorescence quench after subtraction of the nonsaturable component as described in text. (c): Hanes-Woolf plot of data in 6(b)

$\Delta\psi$  develop in the absence of gramicidin. Thus rates measured under these conditions would not reflect initial rates of ATP hydrolysis whereas in the presence of gramicidin the ATPase is unencumbered by the development of  $\Delta\text{pH}$  or  $\Delta\psi$  and the measured rates would reflect initial rates of ATP hydrolysis and so should be comparable to initial rates of  $\text{H}^+$  transport. The close agreement in  $K_m$  values for  $\text{Cl}^-$  stimulation of  $\text{H}^+$  transport and ATPase activity suggest that the saturable component of

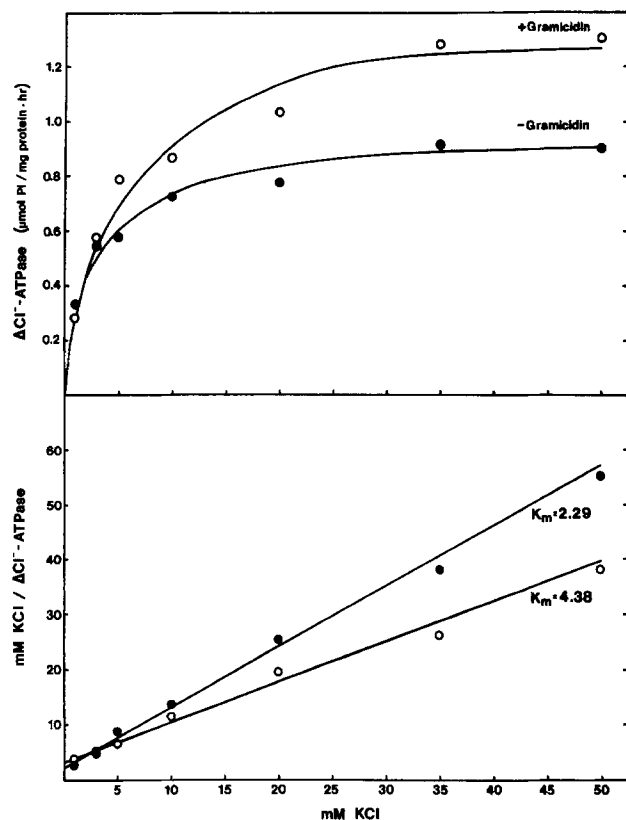


Fig. 8. Kinetics of KCl stimulation of ATPase activity in the presence and absence of gramicidin. ATPase activity was assayed as in Materials and Methods. KCl-stimulated activity calculated as the difference in the activity measured in the presence of 5 mM  $\text{MgSO}_4$  and that measured in the presence of 5 mM  $\text{MgSO}_4$  + KCl. Lower panel shows Hanes-Woolf plot of the same data

$\text{Cl}^-$  stimulated  $\text{H}^+$  transport was due to saturable binding and activation of the  $\text{H}^+$ -ATPase.

#### Effects of $\text{Cl}^-$ on $\Delta\psi$

In order to understand the role of  $\text{Cl}^-$  in the stimulation of  $\text{H}^+$  transport it was necessary to investigate the electrogenic properties of the  $\text{H}^+$ -ATPase in these vesicles. An optical probe of positive interior membrane potentials was used. Oxonol dyes are a class of permeant anions which have been shown to respond rapidly and quantitatively to positive interior membrane potentials (Bashford, Chance & Prince, 1979; Scherman & Henry, 1980). OX-VI has been shown to be the most sensitive of this class of dyes (Bashford & Thayer, 1977) and so was employed here. The response to oxonol dyes apparently depends on shifts between the free and membrane-bound dye and as such, their response is sensitive to the vesicle/dye ratio. Figure 1 shows the response of 2.5  $\mu\text{M}$  OX-VI,

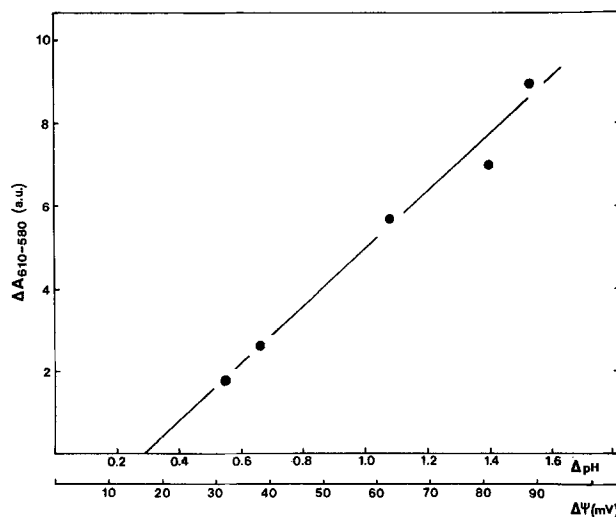
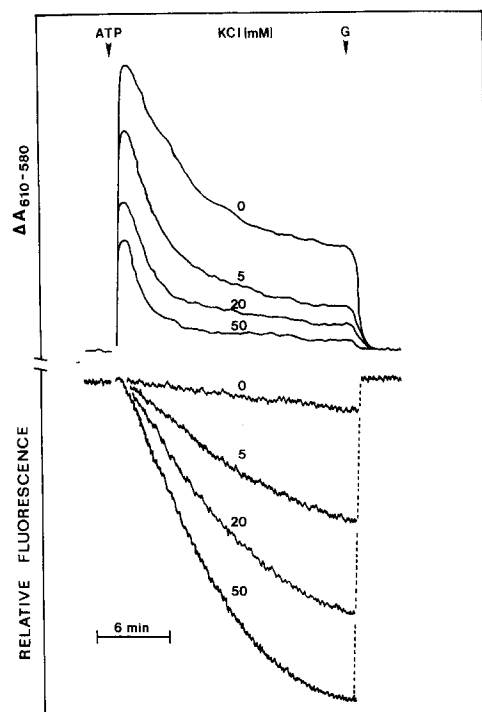


Fig. 9. Calibration curve for OX-VI response to positive interior,  $\text{H}^+$  diffusion potentials. Experimental conditions were as in Fig. 2 except that 2  $\mu\text{M}$  gramicidin was present and changes in  $A_{(610-580)}$  were initiated by the addition of 2–20  $\mu\text{l}$  0.5 N  $\text{H}_2\text{SO}_4$ . No monovalent cations, other than  $\text{H}^+$ , were present. The imposed pH gradient was calculated by measuring the pH in the cuvette before and after addition of  $\text{H}_2\text{SO}_4$

measured as a shift in  $A_{(610-580)}$ , upon the addition of 5 mM ATP at increasing concentrations of membrane protein. The response of the dye saturates at about 60  $\mu\text{g}$  membrane protein/ml. These measurements were made under conditions favoring maximal generation of  $\Delta\psi$  (i.e. no monovalent ions). Since all treatments tested would tend to reduce  $\Delta\psi$ , a concentration of membrane protein in the upper range of the linear region of probe response yielded the highest probe signal, while still remaining responsive to changes in  $\Delta\psi$ . Typically, 50–60  $\mu\text{g}$  membrane protein/ml were used in subsequent experiments.

Preliminary experiments with sonicated liposomes (soybean phospholipids) indicated that the dye could be calibrated with imposed  $\text{K}^+$  gradients and valinomycin and that the response under those conditions was linear to about +150 mV. Attempts to calibrate corn root membrane vesicles by this same method were unsuccessful. It was found that valinomycin increased the conductance of the membrane only at concentrations exceeding 1  $\mu\text{M}$ , a concentration at which valinomycin increased the membrane permeability to  $\text{H}^+$  as well as  $\text{K}^+$  in these membranes. Calibration of the dye was achieved by imposing a pH gradient (acid exterior) in the presence of 2  $\mu\text{M}$  gramicidin and no other monovalent cations. The pH gradient was imposed by the addition of  $\text{H}_2\text{SO}_4$  to a





**Fig. 10.** Time course of the change in  $A_{(610-580)}$  of OX-VI and fluorescence quenching of quinacrine upon the addition of ATP at various concentrations of KCl. Absorbance changes of OX-VI and fluorescence quenching were measured as in Figs. 1 and 2. KCl was present at the concentrations indicated in the Figure. ATP and gramicidin (G) were added to final concentrations of 5 mM and  $2\mu\text{M}$ , respectively, at the indicated points

vesicle suspension equilibrated at pH 6.75, and the shift of  $A_{(610-580)}$  of OX-VI recorded. The results are shown in Fig. 9 where it is apparent that the dye response was linear to at least +90 mV. Upon the addition of ATP, in the absence of  $\text{Cl}^-$ , the shift in  $A_{(610-580)}$  was slightly beyond the range of the calibration curve but indicated the formation of  $\Delta\psi$  of approximately +100 mV (*data not shown*).

The time course of the ATP-dependent shift in  $A_{(610-580)}$  at various  $\text{Cl}^-$  concentrations is shown in the upper panel of Fig. 10. In the lower panel, the quenching of quinacrine fluorescence is shown at the same  $\text{Cl}^-$  concentrations. Both the ATP-dependent shift in  $A_{(610-580)}$  and ATP-dependent quenching of quinacrine fluorescence were reversed by  $2\mu\text{M}$  gramicidin. Figure 11 shows a plot of the maximum shift in  $A_{(610-580)}$  and the initial rate of fluorescence quenching of 9-aminoacridine (data from Fig. 6a) as a function of  $\text{Cl}^-$  concentration. The kinetics of  $\text{Cl}^-$  inhibition of  $\Delta\psi$  show the same biphasic form as previously described for  $\text{Cl}^-$  stimulation of initial rates of  $\text{H}^+$  transport. This result indicates that  $\text{Cl}^-$

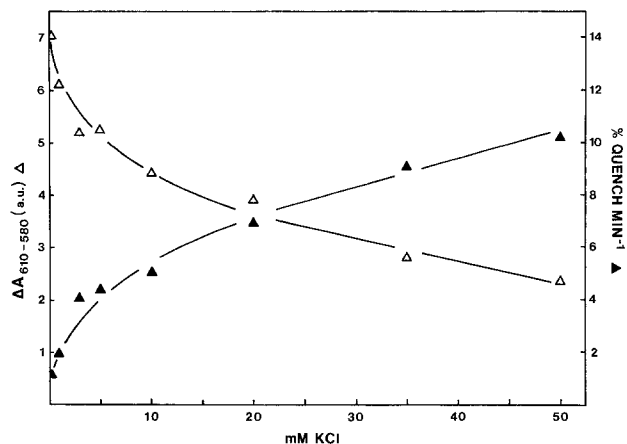


**Fig. 11.** Effects of KCl on the initial rates of fluorescence quenching of 9-aminoacridine (▲) and absorbance changes of OX-VI (Δ). Experimental conditions as in Figs. 1 and 2 except that KCl concentration varied as indicated

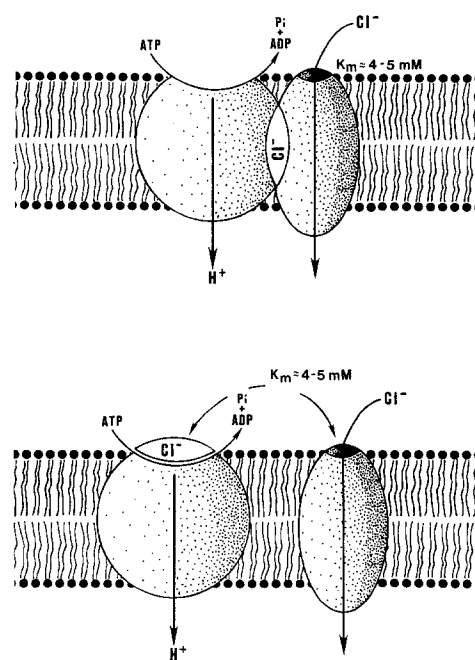


**Fig. 12.** Proposed models of the interaction between the  $\text{H}^+$ -ATPase and an anion channel. The upper model accounts for similarities in kinetic constants for  $\text{Cl}^-$  stimulation of  $\text{H}^+$ -ATPase activity and  $\text{Cl}^-$  stimulation of  $\text{H}^+$  transport by a physical association of the  $\text{H}^+$ -ATPase with a  $\text{Cl}^-$  channel. The lower model accounts for the observed similarities by coincidence. These are not meant to imply a knowledge of the actual physical structure of either the  $\text{H}^+$ -ATPase or anion channel

does stimulate  $\text{H}^+$  transport as a permeant anion at all concentrations tested. The linear component of the apparent  $\text{Cl}^-$  permeation could be explained by a passive permeation of the membrane by  $\text{Cl}^-$  and the saturable com-

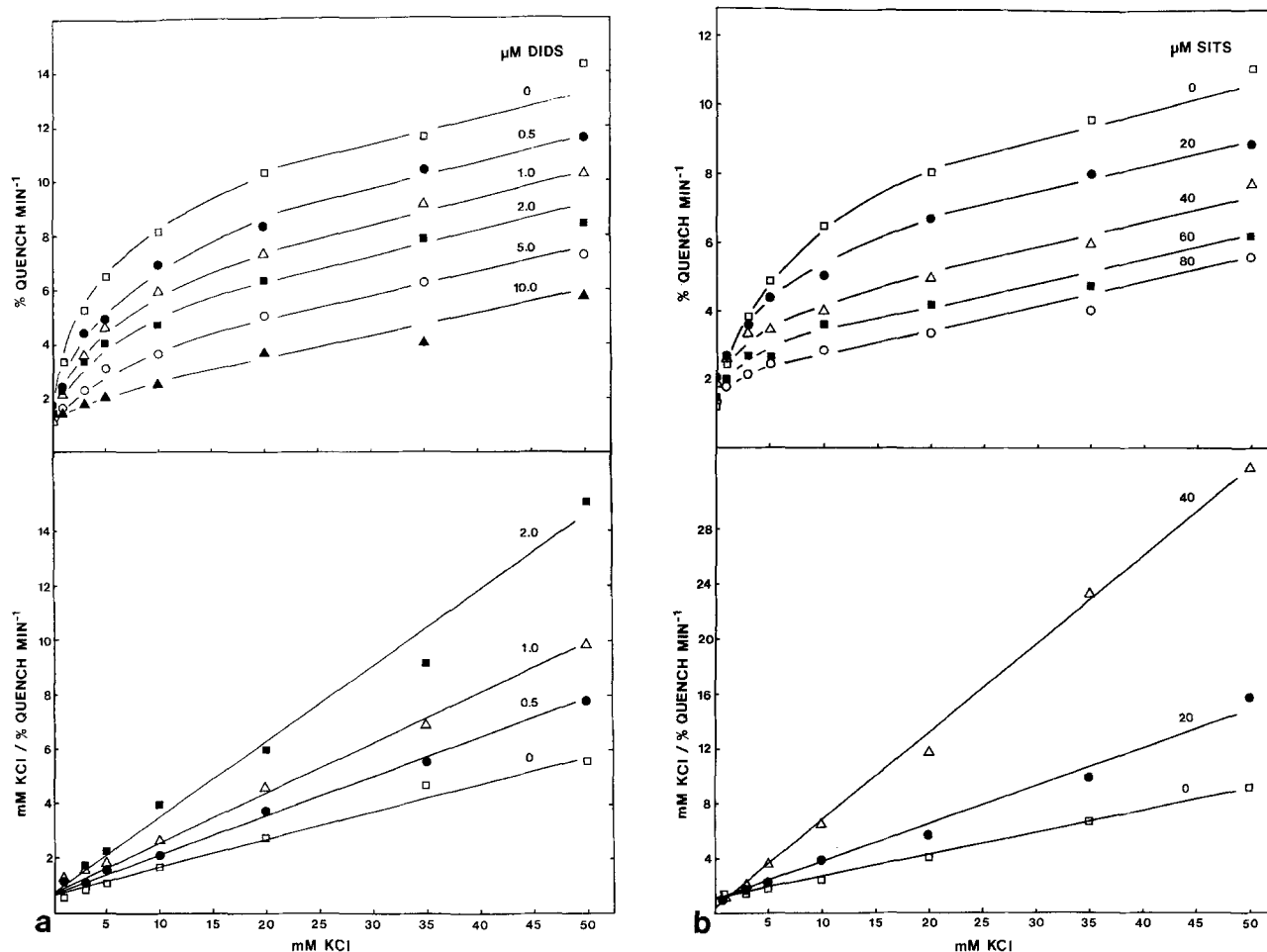


**Fig. 13.** (a): Kinetics of  $\text{Cl}^-$  stimulation of initial rate of fluorescence quenching of quinacrine in the presence of various concentrations of DIDS. Assay conditions as in Fig. 1 with additions of DIDS to the final concentrations indicated in the Figure. Lower panel shows a Hanes-Woolf plot of the saturable component of  $\text{Cl}^-$ -stimulated fluorescence quenching after subtraction of the nonsaturable component as described in the text. (b): Exactly as 13 (a) except that SITS replaced DIDS

ponent explained by permeation through an anion channel.

In order to reconcile the observations that  $\text{Cl}^-$  directly activates the  $\text{H}^+$ -ATPase, stimulates  $\text{H}^+$  transport, and relieves  $\Delta\psi$  with similar kinetics, two models are proposed in Fig. 12. In the upper model an anion channel is physically associated with the  $\text{H}^+$ -ATPase and the site for  $\text{Cl}^-$  activation of the  $\text{H}^+$ -ATPase is accessible only to  $\text{Cl}^-$  inside the channel. The kinetic constant associated with entry into the channel would then determine the kinetics of  $\text{Cl}^-$  stimulation of the  $\text{H}^+$ -ATPase as well as the saturable component of  $\text{Cl}^-$  permeation of the membrane, and its consequent effect on  $\Delta\psi$  and rates of  $\text{H}^+$  transport. The lower model proposes that the anion channel and  $\text{H}^+$ -ATPase are not physically associated, that the site for

$\text{Cl}^-$  activation of the  $\text{H}^+$ -ATPase is accessible to  $\text{Cl}^-$  in free solution and that kinetic constants associated with  $\text{Cl}^-$  entry into the anion channel and  $\text{Cl}^-$  stimulation of the  $\text{H}^+$ -ATPase are similar by coincidence. In both models the linear component of  $\text{Cl}^-$  stimulation of  $\text{H}^+$  transport is assumed to be explained by passive permeation of the membrane by  $\text{Cl}^-$ .

#### *Effect of SITS and DIDS on $\text{H}^+$ Transport and $\text{H}^+$ -ATPase Activity*

The upper model in Fig. 12 is similar to one proposed for the chromaffin granule  $\text{H}^+$ -ATPase (Pazoles, Creutz, Ramu & Pollard, 1980). In that system it was found that an anion channel blocker, 4-acetamido-4'-isothiocyano-2,2'-stilbenedisulfonic acid (SITS),

**Table 2.** Effect of SITS on ATPase activity<sup>a</sup>

Additions (M)	ATPase activity ( $\mu\text{mol Pi/mg} \cdot \text{hr}$ )			%Inhi- bition of $\text{Cl}^-$ - ATPase
	– KCl	+ KCl	$\text{Cl}^-$ stimu- lation	
– Gramicidin				
0 SITS	1.48	1.97	0.49	–
40 SITS	0.74	1.17	0.40	19.0
80 SITS	0.52	0.84	0.32	34.5
+ Gramicidin				
0 SITS	2.46	3.15	0.70	–
40 SITS	1.07	1.83	0.76	–8.6
80 SITS	0.64	1.27	0.62	10.3

<sup>a</sup> ATPase activity assayed as in Materials and Methods with SITS added at the indicated concentration. Mg-ATPase is calculated as the difference in ATPase activity measured in the presence and absence of 5 mM  $\text{MgSO}_4$ . Gramicidin, when present, was added at a final concentration of 2  $\mu\text{M}$

inhibited the  $\text{H}^+$ -ATPase even after solubilization of the enzyme. Figure 13 shows the effects of two well-known anion channel blockers, 4,4'-diisothiocyano-2,2'-stilbenedisulfonic acid (DIDS) and SITS, on the kinetics of  $\text{Cl}^-$  stimulation of  $\text{H}^+$  transport, measured as the initial rates of fluorescence quenching of quinacrine. In both cases it is apparent that these inhibitors had no effect on the linear component of  $\text{Cl}^-$  stimulation of  $\text{H}^+$  transport but 10  $\mu\text{M}$  DIDS and 80  $\mu\text{M}$  SITS almost completely abolished the saturable component. The lower panels of Fig. 13 show Hanes-Woolf plots of the saturable components of  $\text{Cl}^-$  stimulated  $\text{H}^+$  transport at the indicated concentrations of DIDS or SITS. In both cases the kinetics indicated uncompetitive inhibition (Segel, 1975). These results support the contention that a  $\text{Cl}^-$  channel is responsible for the saturable component of  $\text{Cl}^-$  stimulated  $\text{H}^+$  transport but it did not help distinguish between the two models shown in Fig. 12.

The effects of SITS on ATPase activity were also determined (Table 2). In the absence of gramicidin the  $\text{Cl}^-$  stimulated ATPase activity was inhibited approximately 34%. However, in the presence of gramicidin the  $\text{Cl}^-$  stimulated ATPase activity was affected little, if at all, even at concentrations which completely abolished the saturable component of  $\text{Cl}^-$  stimulated  $\text{H}^+$  transport. Similar results were obtained with DIDS. This result indicated that even at concentrations of SITS which completely blocked the saturable component of  $\text{Cl}^-$  permeation,

the site for activation of the  $\text{H}^+$ -ATPase was still accessible to  $\text{Cl}^-$ . While this result tends to support the lower model of Fig. 12, it could equally well be explained if SITS blocked exit from the anion channel but not entry into it. Since the detailed mechanism of SITS inhibition is not known, a distinction between these two models cannot be made.

## Conclusions

Previous characterization of ATP-dependent  $\text{H}^+$  transport in plant cell microsomal vesicles in this laboratory (DuPont et al., 1982c) and others (Stout & Cleland, 1982) has indicated that  $\text{H}^+$  transport and associated ATPase activity was stimulated by anions. It has been suggested that this stimulation occurred by virtue of electrical coupling between anion and  $\text{H}^+$  fluxes (DuPont et al., 1982c). This contention is supported by the data presented here that  $\text{Cl}^-$  relieved  $\Delta\psi$  with the same kinetics that  $\text{Cl}^-$  stimulated  $\text{H}^+$  transport. The further observation, however, that  $\text{Cl}^-$  stimulated ATPase activity even in the presence of 2  $\mu\text{M}$  gramicidin indicated that  $\text{Cl}^-$  had an additional role in directly activating the  $\text{H}^+$ -ATPase. This dual role of  $\text{Cl}^-$  suggests that the  $\text{H}^+$ -ATPase may catalyze the nearly electro-neutral transport of  $\text{H}^+$  and  $\text{Cl}^-$  (or other anions) under physiological conditions.

The similarity in kinetic constants for the saturable component of  $\text{Cl}^-$  stimulated  $\text{H}^+$  transport, inhibition of  $\Delta\psi$ , and  $\text{Cl}^-$  stimulated ATPase activity suggests that there is a common rate-limiting step in these processes. This common reaction may involve entry of  $\text{Cl}^-$  to an anion channel which is physically associated with the  $\text{H}^+$ -ATPase. Such a physical association of an  $\text{H}^+$ -ATPase with an anion channel has been proposed for the chromaffin granule  $\text{H}^+$ -ATPase (Pazoles et al., 1980). The similarities in kinetic constants, may, however, be coincidental and the model of a true physical association between the  $\text{H}^+$ -ATPase and an anion channel must remain tentative. Solubilization and reconstitution of an active  $\text{Cl}^-$  stimulated  $\text{H}^+$ -ATPase will hopefully clarify this point.

We would like to thank Dr. R.K. Clayton for use of the dual wavelength spectrophotometer, Dr. F.M. DuPont for critical reading of the manuscript, and D. Giorgi for technical assistance.

This work was supported by NSF grant PCM 78-12119 to R.M.S.

## Appendix

We have used initial rates of fluorescence quench ( $\% Q \text{ min}^{-1}$ ) to compare relative initial rates of  $\text{H}^+$  influx into membrane vesicles. The justification that the rate of quench is proportional to the rate of  $\text{H}^+$  influx is as follows:

The net change in internal pH, which is equivalent to the net flux of protons and hydroxyls (see Nichols, Hill, Bangham & Deamer, 1980) can be written as:

$$J_{\text{net}} = \frac{-d\text{pH}_{\text{in}}}{dt} B_i V_i / A$$

or in terms of internal proton concentration ( $[\text{H}^+]_{\text{in}}$ ) as:

$$J_{\text{net}} = (B_i V_i / 2.303 [\text{H}^+]_{\text{in}} A) \frac{d[\text{H}^+]_{\text{in}}}{dt} \quad (\text{A1})$$

where  $B_i$  and  $V_i$  are the internal buffering capacity and internal vesicular volume, respectively, and  $A$  is the surface area of the vesicles. As written, a positive flux denotes net proton flux into vesicles.

Rearranging Eq. (2) (Fig. 3) and taking antilogs gives:

$$[\text{H}^+]_{\text{in}} / [\text{H}^+]_{\text{out}} = (\%Q / 100 - \%Q) V_i / V_o$$

which, assuming that  $[\text{H}^+]_{\text{out}}$  is constant, can be differentiated with respect to time to give:

$$\frac{d[\text{H}^+]_{\text{in}}}{dt} = [\text{H}^+]_{\text{out}} (V_i / 100 V_o) \frac{d\%Q}{dt} \quad (\text{A2})$$

Substituting Eq. (A2) into Eq. (A1) gives:

$$J_{\text{net}} = [\text{H}^+]_{\text{out}} / [\text{H}^+]_{\text{in}} (B_i V_i^2 / 230.3 A V_o) \frac{d\%Q}{dt}.$$

Initially  $[\text{H}^+]_{\text{out}} = [\text{H}^+]_{\text{in}}$ , so the initial net flux is given by:

$$J_{\text{net}} = (B_i V_i^2 / 230.3 A V_o) \frac{d\%Q}{dt} \quad (\text{A3})$$

Initially the passive  $\text{H}^+$  efflux is zero so the initial  $\text{H}^+$  flux ( $J_{\text{net}}$ ) is equal to the  $\text{H}^+$  flux through the pump. As shown by Eq. (A3) this initial  $\text{H}^+$  flux is proportional to the initial rate of fluorescence quench under conditions where the vesicular volume is constant.

## References

- Ames, B.N. 1966. Assay of inorganic phosphate, total phosphate and phosphatase. *Methods Enzymol.* **8**:115-118
- Bashford, C.L., Chance, B., Prince, R.C. 1979. Oxonol dyes as monitors of membrane potential. Their behavior in photosynthetic bacteria. *Biochim. Biophys. Acta* **545**:46-57
- Bashford, C.L., Thayer, W.S. 1977. Thermodynamics of electrochemical proton gradient in bovine heart sub-mitochondrial particles. *J. Biol. Chem.* **252**:8459-8463
- Bradford, M.M. 1976. A rapid and sensitive method for the quantitation of microgram quantities of protein utilizing the principle of protein-dye binding. *Anal. Biochem.* **72**:248-254
- Brey, N.R., Rosen, B.P. 1979. Cation/proton antiport systems in *Escherichia coli*. Properties of the calcium/proton antiporter. *J. Biol. Chem.* **254**:1957-1963
- Cohen, S.R. 1975. A comparison of the rate equations, kinetic parameters and activation energies for the initial uptake of L-lysine, L-valine,  $\alpha$ -aminobutyric acid, and  $\alpha$ -aminoisobutyric acid by mouse brain slices. *J. Membrane Biol.* **22**:53-60
- Deamer, D.W., Prince, R.C., Crofts, A.R. 1972. The response of fluorescent amines to pH gradients across liposome membranes. *Biochim. Biophys. Acta* **274**:323-335
- DuPont, F.M., Bennett, A.B., Spanswick, R.M. 1982a. Proton transport in membrane vesicles from corn roots. In: Plasmalemma and Tonoplast: Their Functions in the Plant Cell. D. Marmé, E. Marré, and R. Hertel, editors. pp. 409-416. Elsevier Biomedical Press, Amsterdam
- DuPont, F.M., Bennett, A.B., Spanswick, R.M. 1982b. Localization of a proton-translocating ATPase on sucrose gradients. *Plant Physiol. (in press)*
- DuPont, F.M., Giorgi, D., Spanswick, R.M. 1982c. Characterization of a proton-translocating ATPase in microsomal vesicles from corn roots. *Plant Physiol. (in press)*
- Hager, A., Frenzel, R., Laible, D. 1980. ATP-dependent proton transport into vesicles of microsomal membranes of *Zea mays* coleoptiles. *Z. Naturforsch.* **35c**:783-793
- Lee, H.C., Forte, J.G. 1978. A study of  $\text{H}^+$  transport in gastric microsomal vesicles using fluorescence probes. *Biochim. Biophys. Acta* **508**:339-359
- Lee, H.C., Forte, J.G., Epel, D. 1982. The use of fluorescent amines for the measurement of pH: Applications in liposomes, gastric microsomes, and sea urchin gametes. In: Intracellular pH: Its Measurement, Regulation, and Utilization in Cellular Functions. R. Nuccitelli and D.W. Deamer, editors. pp. 136-158. Alan R. Liss, New York
- Mettler, I.J., Mandala, S., Taiz, L. 1982. Proton gradients produced *in vitro* by microsomal vesicles from corn coleoptiles. Tonoplast origin? In: Plasmalemma and Tonoplast: Their Functions in the Plant Cell. D. Marmé, E. Marré, and R. Hertel, editors. pp. 395-400. Elsevier Biomedical Press, Amsterdam
- Nichols, J.W., Hill, M.W., Bangham, A.D., Deamer, D.W. 1980. Measurement of net proton-hydroxyl permeability of large unilamellar liposomes with the fluorescent pH probe, 9-aminoacridine. *Biochim. Biophys. Acta* **596**:383-403
- Pazoles, C.J., Creutz, C.E., Ramu, A., Pollard, H.B. 1980. Permeant anion activation of MgATPase activity in chromaffin granules. Evidence for direct coupling of proton and anion transport. *J. Biol. Chem.* **255**:7863-7869
- Perlin, D.S., Spanswick, R.M. 1982. Isolation and assay of plasma membrane vesicles from corn root with reduced proton permeability. *Biochim. Biophys. Acta* **690**:178-186
- Rasi-Caldogno, F., DeMichelis, M.I., Pugliarello, M.C. 1981. Evidence for an electrogenic ATPase in microsomal vesicle from pea internodes. *Biochim. Biophys. Acta* **642**:37-45
- Segel, I.H. 1975. Enzyme Kinetics. pp. 210-212. John Wiley & Sons, New York
- Scherman, D., Henry, J.P. 1980. Oxonol-V as a probe of chromaffin granule membrane potentials. *Biochim. Biophys. Acta* **599**:150-166

- Schuldiner, S., Rottenberg, H., Avron, M. 1972. Determination of  $\Delta\text{pH}$  in chloroplasts. 2. Fluorescent amines as a probe for the determination of  $\Delta\text{pH}$  in chloroplasts. *Eur. J. Biochem.* **25**:64-70
- Stout, R.G., Cleland, R.E. 1982. Evidence for a  $\text{Cl}^-$  stimulated Mg-ATPase proton pump in oat root membranes. *Plant Physiol.* **69**:798-803
- Sze, H. 1980. Nigericin-stimulated ATPase activity in microsomal vesicles of tobacco callus. *Proc. Natl. Acad. Sci. USA* **77**:5904-5908
- Sze, H., Churchill, K.A. 1981.  $\text{Mg}^{2+}/\text{KCl}$ -ATPase of plant plasma membranes is an electrogenic pump. *Proc. Natl. Acad. Sci. USA* **78**:5578-5582
- Walker, R.R., Leigh, R.A. 1981. Characterization of a salt-stimulated ATPase activity associated with vacuoles isolated from storage roots of red beet (*Beta vulgaris* L.). *Planta* **153**:140-149

Received 30 March 1982; revised 14 July 1982